DOI: 10.1002/chem.200800388

Modular Chiral Bidentate Phosphonites: Design, Synthesis, and Application in Catalytic Asymmetric Hydroformylation Reactions

Baoguo Zhao,[a] Xingao Peng,[a, b] Zheng Wang,[a] Chungu Xia,*[b] and Kuiling Ding*[a]

Dedicated to Professor Xiyan Lu on the occasion of his 80th birthday

Abstract: A new class of C_2-symmetric chiral bidentate phosphonite ligands has been synthesized in moderate to good yields from readily available starting materials. Application of these air-stable chiral phosphonites in the Rh^I-catalyzed asymmetric hydroformylation of styrene derivatives, vinyl acetate, and allyl cyanide afforded the corresponding chiral aldehydes with high regio- and enantioselectivities under mild reaction conditions. The modular nature of the ligands allows fine-tuning of the selectivities through judicious modifications of the substituents on the ligand backbone. X-ray structural analysis of the catalyst precursor suggested that the steric hindrance caused by the protruding remote substituents of the ligands into the vicinity of the metal center might be an important factor for the enantio-control of the reaction, whereas the sense of asymmetric induction can be rationalized on the basis of a trigonal-bipyramidal transition state diagram.

Keywords: asymmetric catalysis · bidentate ligands · hydroformylation · phosphonite ligands · rhodium

Introduction

Hydroformylation (HF)[1] represents one of the most important homogeneously catalyzed industrial processes with millions of tons of oxo products being produced worldwide per year. Catalytic asymmetric hydroformylation (AHF) is an atom-economic one-carbon homologation reaction that converts in a single step olefins and syngas (CO/H_2) into chiral aldehydes, which can be used as important chiral synthons for a variety of pharmaceutical products and fine chemicals.[1–3] Despite the considerable interest from both industry and academia, however, the catalytic AHF is still a challenging area in comparison with the rapid development of other catalytic asymmetric reactions.[4] One of the major problems involved in the reaction is how to control both the regio- and enantioselectivities while maintaining reasonable reaction rates at moderately high temperatures (60–100 °C). This is usually a difficult goal since reduced regio- and enantioselectivities are often obtained at higher temperatures. Although these selectivities can be modulated to some extent by altering reaction parameters, such as gas pressure and reaction temperature, the employed chiral ligand is the most important factor in selectivity control.[2] Therefore, in the area of Rh^I-catalyzed AHF, significant improvements with regard to catalytic activity and/or selectivity have always been closely associated with the successful discovery/development of new ligands. Over the past three decades, although a large variety of chiral ligands has been examined in Rh^I-catalyzed AHF, excellent results have only been reported for a limited number of ligands so far.[2e] Some of the representative ligands are shown in Scheme 1. The catalysis involving chiral bisphosphites **1** and **2** demonstrated some degree of substrate specificity. Whereas the former exhibited good enantioselectivity in the reaction of styrene,[5] the latter was found quite efficient in the stereocontrol of the hydroformylation of allyl cyanide and vinyl acetate.[6] Wills et al. reported the first phospholane-type ligand (**3**) was ef-

[a] Dr. B. Zhao, X. Peng, Prof. Dr. Z. Wang, Prof. Dr. K. Ding
State Key Laboratory of Organometallic Chemistry
Shanghai Institute of Organic Chemistry
Chinese Academy of Sciences
354 Fenglin Road, Shanghai 200032 (China)
Fax: (+86) 216-416-6128
E-mail: kding@mail.sioc.ac.cn

[b] X. Peng, Prof. Dr. C. Xia
State Key Laboratory of Oxo Synthesis and Selective Oxidation
Lanzhou Institute of Chemical Physics
Chinese Academy of Sciences
Lanzhou 730000 (China)
Fax: (+86) 931-827-7088
E-mail: cgxia@lzb.ac.cn

Supporting information for this article is available on the WWW under http://dx.doi.org/10.1002/chem.200800388.

 © 2008 Wiley-VCH Verlag GmbH & Co. KGaA, Weinheim

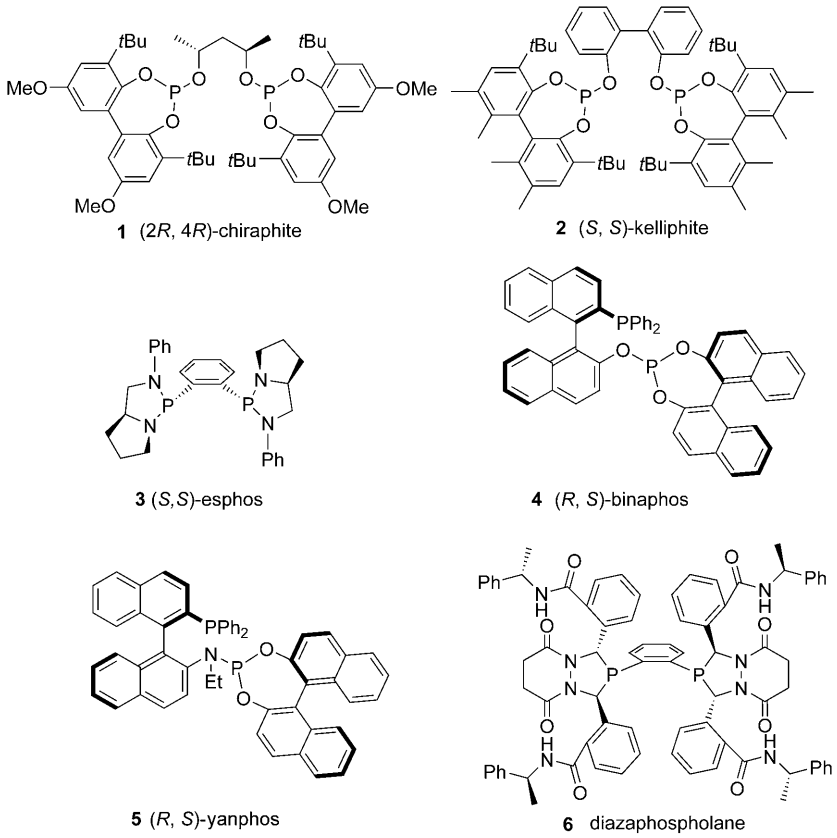

Scheme 1. Representative examples of chiral ligands for Rh^I-catalyzed AHF of olefins.

fective for AHF of vinyl acetate, but quite unselective toward hydroformylation of styrene.[7] The discovery of the Rh/binaphos (**4**) catalysts by Takaya, Nozaki and co-workers in 1993 is widely regarded as a breakthrough in this field. A variety of olefins were hydroformylated with generally high levels of regio- and enantioselectivity using this versatile catalyst.[8] Very recently, Zhang and Yan reported phosphine–phosphoramidite (**5**), a ligand structurally related to (*R*,*S*)-binaphos (**4**) in which an oxygen atom was replaced by an NEt fragment, which significantly improved the enantioselectivities over (*R*,*S*)-binaphos in AHF of vinyl arenes and vinyl acetate[9] The diazaphospholane **6** and its analogues, reported by Klosin and co-workers in 2005, also demonstrated very effective control of regio- and enantioselectivities in the AHF of styrene, vinyl acetate, and allyl cyanide substrates, with remarkable features of high catalytic activity at elevated temperatures.[10] Overall chiral ligands with a new skeleton for this important asymmetric catalytic reaction would be highly desirable.[11] Herein, we report the results on the design and synthesis of a new class of modular C_2-symmetric chiral bidentate phosphonite ligands, as well as their application in the Rh^I-catalyzed asymmetric hydroformylation of styrene derivatives, vinyl acetate, and allyl cyanide with the effective control of the regio- and stereoselectivities. The solid-state structure of the catalyst precursor has also been elucidated to shed some light on the origin of the selectivity control of the reaction.

Results and Discussion

Ligand design: Based on the observation that the phosphites can be highly effective ligands for the reaction with excellent reactivities,[5,6] and that the chiral ligands bearing a 1,2-diphosphinoethane or 1,2-diphosphinobenzene moiety often demonstrated excellent regio- or enantioselective control in the reaction,[6c,7,10,11] it was envisioned that incorporation of both structural features into one ligand molecule might result in a combination of these advantages in a best scenario. During the course of our investigation on modular chiral catalysts for asymmetric catalysis, a wide variety of modular monodentate phosphoramide ligands, DpenPhos (**7**)[12a,b] and CydamPhos (**8**)[12c] based on chiral 1,2-phenylethlene-1,2-diamine and 1,2-diaminocyclohexane, respectively, have been developed. Dual steric tuning of the substituents on the ligands is critically important for achieving excellent enantioselectivity in Rh^I-catalyzed hydrogenations of a variety of functionalized olefin derivatives, such as dehydro-α-amino acid derivatives, enamides, methyl (*Z*)-β-substituted α-acetoxyacrylates, or (*E*)-β-aryl itaconate derivatives. The drastic impact of substituents on the ligands on the enantioselectivity of the reactions can be addressed on the basis of their spatial orientations in the Rh^I complexes, which constitute an integral part of the chiral environment around the Rh^I center. By taking the advantages of the structural diversity and remote stereocontrol capability of the substituents on the backbone of **7** and **8**, the privileged skeleton of 1,2-diphosphinoethane or 1,2-diphosphinobenzene, as well as the high activity of phosphite ligands, we decided to prepare a series of bidentate phosphonite ligands (**9** and **10**) (Scheme 2) containing all of the elements above for the Rh^I-catalyzed AHF reaction of olefin derivatives.

Ligand synthesis: As shown in Scheme 3, the synthesis of modular bidentate phosphonite ligands **9** and **10** was quite straightforward and was accomplished in a convergent manner. The diphenol derivative (*R*,*R*)-**11**, which is a key intermediate in the preparation of DpenPhos and can be readily prepared from (1*R*,2*R*)-1,2-bis(2-methoxyphenyl)ethane-1,2-diamine,[12a–b] was allowed to react with 1,2-bis(dichlorophosphino)ethane (**12**) or 1,2-bis(dichlorophosphino)benzene (**13**) in THF in the presence of Et_3N as HCl scavenger

 © 2008 Wiley-VCH Verlag GmbH & Co. KGaA, Weinheim

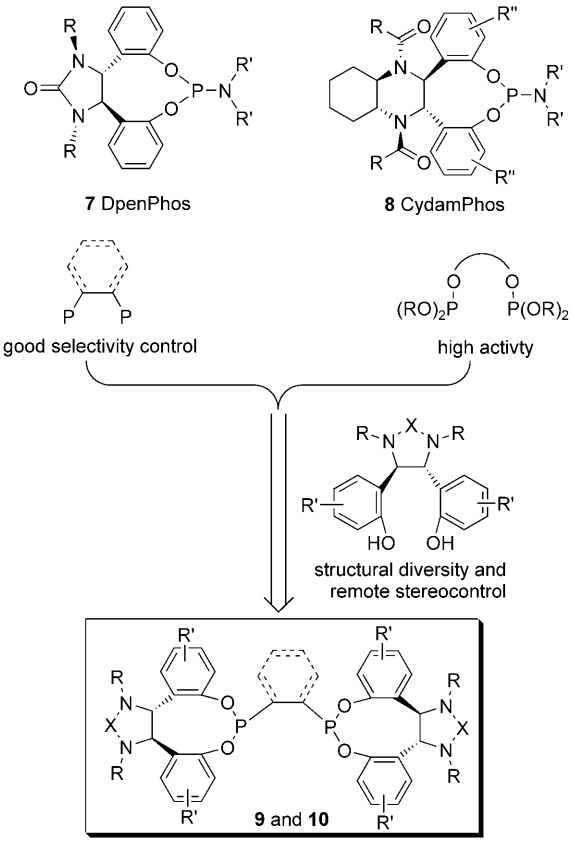

Scheme 2. The concept of ligand design for Rh^I-catalyzed AHF of olefins.

at room temperature. This afforded the corresponding bidentate phosphonite ligands **9a**,**b** having an ethylene and phenylene backbone, respectively, in reasonably good yields (66–71%). These two compounds were purified by column chromatography on silica gel without special precaution against air or trace amounts of water in the solvent. Considering the ready availability and facile modification of diphenol **14**,[12c] we decided to further extend the bisphosphonite ligand diversity with this skeleton. Thus, the key diphenol intermediates **14a–l** were conveniently prepared in good yields (76–85%) from readily available enantiopure 1,2-diaminocyclohexane and various salicylaldehyde derivatives through a three-step reaction sequence developed in our laboratory. Similarly, the reaction of **14** with 0.5 equivalents of **13** in dry THF at room temperature in the presence of 2 equivalents of Et_3N afforded the corresponding bidentate phosphonite ligands **10a–l** in moderate to good yields. These chiral phosphonite ligands were stable enough to allow purification by silica gel column chromatography in the open air, and could be stored under argon without degradation for long periods (>6 months).

Optimization of reaction conditions: With the novel chiral bidentate phosphonite ligands **9a**,**b** and **10a–l** in hand, we then proceeded to examine their asymmetric induction ability in the Rh^I-catalyzed AHF of the three most commonly used model substrates, namely styrene (**15a**), vinyl acetate (**18**), and allyl cyanide (**21**) (Scheme 4). The reaction was performed in a Parr autoclave under a pressure of 20 bar CO/H_2 (1/1) in toluene at 60°C in the presence of 0.2 mol% of Rh^I complexes, and the conversions of the substrates, and the regio- and enantioselectivities of the reactions were determined by GC analysis. The Rh^I complexes were formed in situ by reaction of one equivalent of $[Rh(acac)(CO)_2]$ with 1.5 equivalents of ligands **9** or **10** in toluene. The preliminary examination of the AHF of the substrates with Rh^I complexes of **9a**,**b** indicated that the catalyst composed of ligand **9b** bearing a 1,2-phenylene backbone gave relatively higher regio- and enantioselectivities than that of **9a** with a 1,2-ethylene skeleton (entry 1 vs. 2, Table 1), affording the corresponding branched aldehydes regioselectively with 51–73% *ee*. These results clearly indicate the feasibility of the ligand design concept shown in Scheme 2. Therefore, we subsequently switched our attention to the ligand modification on the basis of the 1,2-phenylene backbone with the readily available diphenols **14** as the chiral modifiers. Accordingly, a family of modular ligands **10a–l** was designed and synthesized as discussed above.

For the optimization of the reaction conditions, ligand **10b** was first chosen to examine various reaction parameters, such as substrate concentration, syngas partial pressure, solvent, temperature, and ligand-to-rhodium ratio. The optimization began with a preliminary examination of the substrate concentration effect on the reactivity/selectivities of the AHF in the presence of the Rh^I/**10b** complex. After screening the concentration ranges from 1.0 to 4.3 M for all three substrates, a concentration of 3.0 M was found to be optimal for both styrene and vinyl acetate, whereas 1.0 M worked best for allyl cyanide (see Table S1 in the Supporting Information). Significant impact of the CO/H_2 partial pressures on the catalytic activities was observed, as reflected in the conversion data listed in Tables S2 and S3 in the Supporting Information. Remarkably, increasing the H_2 partial pressure or lowering the CO partial pressure demonstrated a beneficial effect on the conversions, which is consistent with the mechanistic understanding that an enhanced rate of H_2 oxidation addition to Rh can be expected at higher H_2 pressure, whereas the dissociation of CO from the Rh center to give the active species (dissociation mechanism) would be facilitated under lower CO pressures.[13] Within the pressure range examined for the reactions, 50 atm of H_2/CO (4:1) was found to be optimal for the reaction of styrene and vinyl acetate, whereas 40 atm of 3:1 H_2/CO turned out to be best for the reaction of allyl cyanide with the Rh^I/**10b** system. Subsequent examination of the solvent effects using both ligands **10b** and **10c** under similar conditions revealed that the reactions performed best in *t*BuOMe for all three olefins in terms of the catalytic activities and selectivities (see Table S4 in the Supporting Information).

The impacts of reaction temperature and ligand/Rh ratios on the catalysis are summarized in Table 2. Enhancement of the reaction temperatures from 40 to 60°C led to an improvement of the reaction rate and an essentially constant

 © 2008 Wiley-VCH Verlag GmbH & Co. KGaA, Weinheim

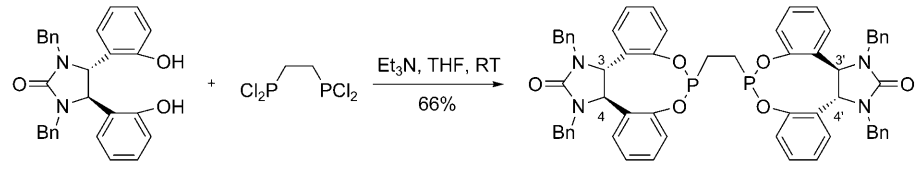

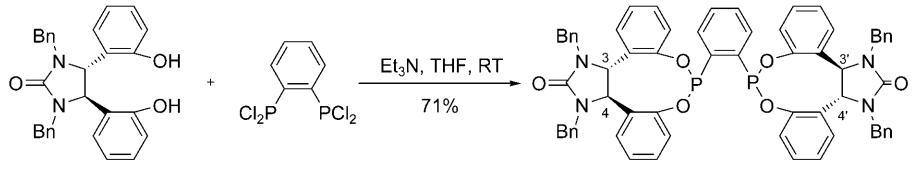

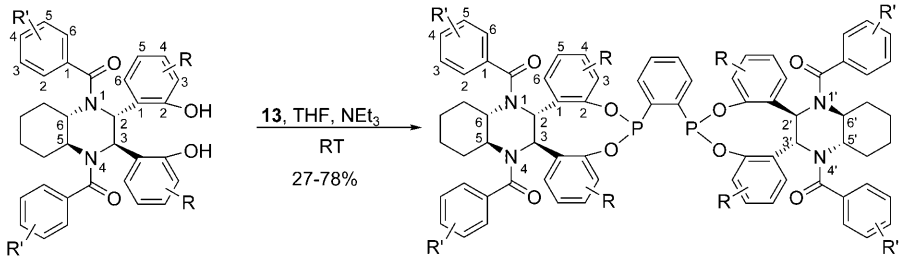

14a: R = H, R' = H
14b: R = H, R' = 4-Me
14c: R = H, R' = 3,5-Me_2
14d: R =3-Me, R' = H
14e: R = 4-Me, R' = H
14f: R = 4-Me, R' = 4-Me
14g: R = 4-Me, R' = 3,5-Me_2
14h: R = 4-*i*Pr, R' = H
14i: R = 4-*t*Bu, R' = H
14j: R = H, R' = 4-Cl
14k: R = H, R' = 4-MeO
14l: R = H, R' = 4-*t*Bu

10a: R = H, R' = H
10b: R = H, R' = 4-Me
10c: R = H, R' = 3,5-Me_2
10d: R =3-Me, R' = H
10e: R = 4-Me, R' = H
10f: R = 4-Me, R' = 4-Me
10g: R = 4-Me, R' = 3,5-Me_2
10h: R = 4-*i*Pr, R' = H
10i: R = 4-*t*Bu, R' = H
10j: R = H, R' = 4-Cl
10k: R = H, R' = 4-MeO
10l: R = H, R' = 4-*t*Bu

Scheme 3. Synthesis of bidentate phosphonite ligands **9** and **10**.

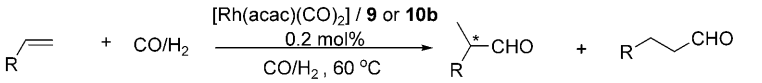

15a: R = Ph
18: R = AcO
21: R = $NCCH_2$

16a: R = Ph
19: R = AcO
22: R = $NCCH_2$

17a: R = Ph
20: R = AcO
23: R = $NCCH_2$

Scheme 4. Rh^I-catalyzed AHF of styrene (**15a**), vinyl acetate (**18**), and allyl cyanide (**21**) in the presence of Rh^I complexes of **9** or **10b**.

ee for all the three substrates, albeit with a slight lowering of b/l ratios (branching/linear ratios; entries 1–3, Table 2). However, a further increase of the temperature to 70 °C resulted in a significant decrease in both regio- and enantioselectivities (entry 4, Table 2). The **10b**/Rh ratios, which can affect the concentrations of the active species through the coordination equilibrium, are found to exhibit a considerable effect on both the regio- and enantioselectivities of the hydroformylations, with a threshold value of 1.5/1 being optimal for all the three substrates (entries 3 and 5–8, Table 2). Further increase of the ligand/Rh^I ratio to 2/1 did not result in much difference in selectivities, albeit with a minor negative effect on the activities. Overall, the optimized conditions turned out to be 50 bar (4:1) or 40 bar (3:1) pressure of H_2/CO for the reaction of styrene/vinyl acetate (3.0 M) or allyl cyanide (1.0 M), respectively, in *t*BuOMe as solvent at 60 °C in the presence of 0.2 mol % of the Rh^I complex of **10b** (1:1.5) for 2 h or 4 h (entry 3, Table 2).

The substituent effect of the ligands: The modular nature of the bidentate chiral phosphonite ligands **10** allows a facile fine-tuning of the catalytic performance through modifications of the stereoelectronic properties of the two sets of substituents on the ligand backbone, R and R′ (Scheme 3). Under the optimized reaction conditions, the impacts of the R and R′ substituents in ligands **10a–l** on the regio- and enantioselectivities were subsequently investigated for the Rh^I-catalyzed asymmetric hydroformylation of vinyl acetate, styrene, and allyl cyanide. As can be seen from Table 3, increasing the steric bulkiness of *N*-arylacyl substituents in the ligand was found to be beneficial to both the regio- and enantioselectivities for all the three kinds of substrates, albeit with a somewhat drop in reactivity for allyl cyanide (entries 1–3, Table 3). For the ligands with R′ = H (**10a**, **10d,e**, and **10h,i**), the steric property of R exhibited a hard-to-predict influence on the regio- and enantioselectivities of the reactions, depending on both the position and the steric bulkiness of R. Whereas modification of the R group at the 3-position from H to Me resulted in considerable degradation in both reactivity and selectivities for the reactions (entry 1 vs. 4, Table 3), the reverse is true for a similar modification at the 4-position on the phenoxy moieties in the ligands (entry 1 vs. 5, Table 3). However, further increasing the steric bulkiness of the 4-substituent by changing Me to *i*Pr or *t*Bu led to somewhat lowered regio- and enantioselectivities of the three reactions (entry 5 vs. 8 and 9, Table 3).

 © 2008 Wiley-VCH Verlag GmbH & Co. KGaA, Weinheim

Table 1. AHF of styrene (**15a**), vinyl acetate (**18**) and allyl cyanide (**21**) under the catalysis of Rh^I/**9a**,**b**.

Entry	**9**	**15a**[a]			**18**[a]			**21**[b]		
		conv. [%][c]	b/l[c]	*ee* [%][c]	conv. [%][c]	b/l[c]	*ee* [%][c]	conv. [%][c]	b/l[c]	*ee* [%][c]
1	**9a**	66	4.5	44.6 (*R*)	82	38	50.0 (*S*)	>99	3.1	44.0 (*R*)
2	**9b**	42	6.3	51.1 (*R*)	27	19.7	51.8 (*S*)	>99	4.4	73.4 (*R*)

[a] Reaction conditions: [Rh]/**9** = 1:1.5, sub./cat. = 500, $P(H_2)$ = 10 bar, $P(CO)$ = 10 bar, [substrate] = 0.68 M, toluene, 60 °C, 5 h. [b] Reaction conditions: [Rh]/**9** = 1:1.5, sub./cat. = 500, $P(H_2)$ = 30 bar, $P(CO)$ = 10 bar, [substrate] = 1.8 M, *t*BuOMe, 60 °C, 4 h. [c] Conversions, branched/linear (b/l) ratios and *ee* values were determined by GC analysis. The absolute configuration for the products **16a**, **19**, and **22** were assigned by comparing the sign of the optical rotations with those in the literature.[18,19]

Table 2. The impact of reaction temperature and ratios of **10b**/[Rh] on the AHF of styrene (**15a**), vinyl acetate (**18**), and allyl cyanide (**21**) in the presence of Rh^I/**10b**.

Entry	**10b**/Rh	*T* [°C]	**15a**[a]			**18**[a]			**21**[b]		
			conv.[%][c]	b/l[c]	*ee* [%][c]	conv. [%][c]	b/l[c]	*ee* [%][c]	conv. [%][c]	b/l[c]	*ee* [%][c]
1	1.5:1	40	29	6.6	66	55	80.0	87	8	3.5	70
2	1.5:1	50	64	5.8	64	71	61.5	87	24	3.4	70
3	1.5:1	60	99	5.7	64	99	36.0	86	99	3.2	73
4	1.5:1	70	99	3.7	51	99	32.3	81	99	3.2	70
5	1.0:1	60	99	7.8	22	99	24.0	71	99	3.3	62
6	1.2:1	60	99	6.7	40	99	26.8	79	99	3.3	66
7	1.8:1	60	99	5.7	63	99	36.0	86	99	3.3	72
8	2.0:1	60	95	5.5	63	94	37.5	86	98	3.3	70

[a] Reaction conditions: sub./cat. = 500, $P(H_2)$ = 40 bar, $P(CO)$ = 10 bar, [substrate] = 3.0 M, *t*BuOMe, 2 h. [b] Reaction conditions: $P(H_2)$ = 30 bar, $P(CO)$ = 10 bar, [substrate] = 1.0 M, 4 h. Other reaction conditions were same as those of [a]. [c] See footnote [c] in Table 1.

Table 3. Rh^I-catalyzed AHF of styrene (**15a**), vinyl acetate (**18**), and allyl cyanide (**21**) in the presence of various ligands **10a–l**.

Entry	Ligand[a]	**15a**[b]			**18**[b]			**21**[c]		
		conv. [%][d]	b/l[d]	*ee* [%][d]	conv. [%][d]	b/l[d]	*ee* [%][d]	conv. [%][d]	b/l[d]	*ee* [%][d]
1	**10a**	99	7.8	56 (*R*)	97	38.5	81 (*S*)	99	4.1	55 (*R*)
2	**10b**	99	5.7	64 (*R*)	99	36.0	86 (*S*)	99	3.2	73 (*R*)
3	**10c**	**99**	**12.2**	**79 (*R*)**	**99**	**40.7**	**91 (*S*)**	80	3.2	77 (*R*)
4	**10d**	42	4.2	6 (*R*)	66	15.3	71 (*R*)	88	0.9	30 (*S*)
5	**10e**	99	15.3	71 (*S*)	99	42.1	88 (*R*)	37	3.8	71 (*S*)
6	**10f**	99	9.2	56 (*S*)	99	37.5	88 (*R*)	40	2.9	68 (*S*)
7	**10g**	95	13.5	37 (*S*)	85	34.5	72 (*R*)	99	2.9	62 (*S*)
8	**10h**	97	16.9	35 (*S*)	81	29.3	63 (*R*)	99	3.8	48 (*S*)
9	**10i**	98	16.8	20 (*S*)	83	19.0	54 (*R*)	99	3.3	26 (*S*)
10	**10j**	99	7.1	46 (*R*)	99	32.3	80 (*S*)	**99**	**4.4**	**79 (*R*)**
11	**10k**	98	6.3	59 (*R*)	93	34.7	84 (*S*)	99	4.2	77 (*R*)
12	**10l**	99	6.4	50 (*R*)	99	23.4	75 (*S*)	99	2.4	56 (*R*)

[a] The configuration of ligands **10a–c** and **10j–l** is (2*R*,3*R*,5*S*,6*S*,2′*R*,3′*R*,5′*S*,6′*S*); the configuration of **10d–i** is (2*S*,3*S*,5*R*,6*R*,2′*S*,3′*S*,5′*R*,6′*R*). [b] Reaction conditions: [Rh]/**10** = 1:1.5, sub./cat. = 500, $P(H_2)$ = 40 bar, $P(CO)$ = 10 bar, [substrate] = 3.0 M, *t*BuOMe, 60 °C, 2 h. [c] Reaction conditions: [Rh]/**10** = 1:1.5, sub./cat. = 500, $P(H_2)$ = 30 bar, $P(CO)$ = 10 bar, [substrate] = 1.0 M, *t*BuOMe, 60 °C, 4 h. [d] See footnote [c] in Table 1.

In the case of R = 4-Me, increasing the steric bulkiness of the *N*-acylaryl group is unfavorable for the reactions, and generally leads to deterioration in both the reactivity and selectivities (entries 5–7, Table 3). Intriguingly, for ligands with R = H, changing the 4-R′ from Me to *t*Bu gave rise to lower catalytic performance (entry 2 vs. 12). Moreover, modification of 4-R′ by changing from H to the electron-withdrawing chloro substituent led to a slight lowering of the selectivities for the reactions of styrene and vinyl acetate. On the other hand, for the ligand with R′ = 4-MeO, the reverse is true (entries 1 vs. 10 and 11, Table 3). For the reaction involving allyl cyanide, both substituents are beneficial to the selectivity control (entries 1 vs. 10 and 11, Table 3). In short, these observations suggested that the stereocontrol capabilities of ligands **10** are highly sensitive to the subtle changes in the structural moieties (R, R′). This can be better understood by a closer examination of the X-ray single-crystal structure of the catalyst precursor [Rh(2*R*,3*R*,5*S*,6*S*,2′*R*,3′*R*,5′*S*,6′*S*)-**10b**(acac)] (Figure 1). Remarkably, whereas the R groups are spatially located near to the reaction site and are expected to exert influences on the reaction, two of the four R′ groups bonded remotely at the ligand backbone, also exhibit a similar spatial orientation. A complex interaction of these factors seems to play a key role in determining the catalytic performance of the Rh complex. These facts along with the modular nature of this type of ligands suggest that their asymmetric induction capabilities in AHF could be readily tuned by judicious modifications of the R and R′ substituents on the skeleton of the ligands, which represents a valuable feature for ligand optimization. Within the ligand series, **10c** turns out to be the best for AHF of vinyl acetate (up to 91% *ee* with b/l = 40.7) and styrene (up to 79% *ee* with b/l = 12.2) in terms of regio- and enantioselectivity, whereas **10j** is optimal for the reaction of allyl cyanide (up to 79% *ee* with b/l = 4.4).

Substrate adaptability: To investigate the substrate adaptability of the Rh^I catalyst containing ligand **10c**, a series of olefin derivatives was hydroformylated in the presence of [Rh(acac)$(CO)_2$]/**10c** under the optimized reaction conditions. These afforded the corresponding products in moderate to excellent regioselectivities and enantioselectivities (entries 1–7, Table 4). Remarkably, hydroformylation of vinyl acetate using the Rh^I/**10c** catalyst demonstrated high reactivity (92% conversion after 12 h) and excellent regio- (b/l = 44.5) and enantioselectivity (90% *ee*) (entry 8,

 © 2008 Wiley-VCH Verlag GmbH & Co. KGaA, Weinheim

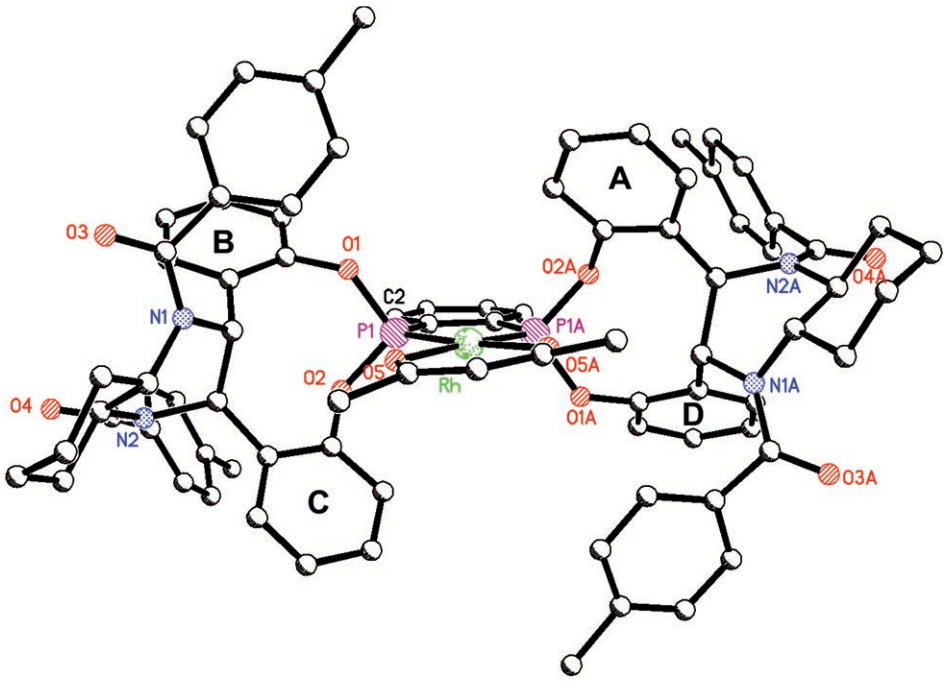

Figure 1. Structure of complex [Rh(2*R*,3*R*,5*S*,6*S*,2′*R*,3′*R*,5′*S*,6′*S*)-**10b**(acac)]. The hydrogen atoms are omitted for clarity. Selected interatomic distances [Å], and angles and torsion angles [°] in the complex: Rh–P1 2.1212(15), P1–O1 1.610(4), P1–O2 1.632(4), P1–C1 1.818(5); P1-Rh-P1A 84.42(9), O1-P1-O2 101.3(2), O1-P1-C1 105.5(2), O2-P1-C1 99.7(2), O1-P1-Rh 112.33(17), O2-P1-Rh 121.56(15), C1-P1-Rh, 114.35(17), O5-Rh-P1-O1 64.1(2), O5-Rh-P1-O1 62(2), P1-Rh-P1-O1 119.22(18).

Table 4. AHF of olefins under the catalysis of optimized catalyst Rh(I)/**10c** or Rh(I)/**10j**.[a]

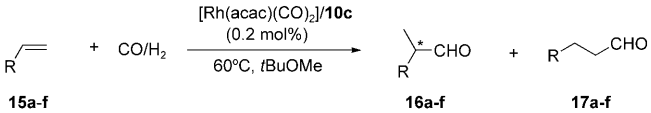

15a-f **16a-f** **17a-f**
18 **19** **20**
21 **22** **23**

Entry	R	Conv. [%]	b/l	*ee* [%][d]
1	C_6H_5 (**15a**)	99	12.2	79 (*R*)
2	4-FC_6H_5 (**15b**)	99	10.9	68 (–)
3	4-MeC_6H_5 (**15c**)	98	9.9	75 (–)
4	4-$MeOC_6H_5$ (**15d**)	87	9.1	72 (–)
5	6-$MeOC_{10}H_6$ (**15e**)	99	8.9	70 (–)
6	AcO (**18**)	99	40.7	91 (*S*)
7[b]	$NCCH_2$ (**21**)	99	4.4	79 (*R*)
8[c]	AcO (**18**)	92	44.5	90 (*S*)

[a] Unless otherwise noted, the reaction conditions are identical to those in Table 3. [b] Ligand **10j** is used. $P(H_2)=30$ bar, $P(CO)=10$ bar. [c] Substrate/Rh = 10000/1, $t=12$ h. [d] The absolute configurations for the products were assigned by comparing the signs of their optical rotations with those in the literature.[18,19]

Table 4) under a low catalyst loading (substrate/catalyst = 10000/1).

Crystal structure of the catalyst precursor [Rh(10b)(acac)]: To probe the origin of the selectivity control of the present catalyst system, we succeeded in obtaining the single crystals of the catalyst precursor [Rh(**10b**)(acac)], by vapor-phase diffusion of hexane into an equimolar solution of [Rh(acac)$(CO)_2$] and **10b** in chloroform at room temperature. X-ray crystallographic analysis (Figure 1) revealed that [Rh(**10b**)(acac)] is C_2 symmetric in its solid state, with a square-planar coordination geometry around the Rh center. The value of the P1-Rh-P1A bite angle is 84.42°, which is close to an inherent bite angle of 90° for four-coordinate Rh complexes.[6c] The rigid 1,2-diphosphinobenzene moiety formed a five-membered ring by the chelating coordination of phosphorus atoms with the Rh atom, whereas the phenoxy rings A and C are close to the catalytic active site (Rh center), and thus are expected to exert an impact on both reactivity and selectivities. Interestingly, the *N*-acyl aromatic rings, located at the "remote" site of the ligand backbone, were also found to protrude into the vicinity of the Rh center by virtue of the orientation of the acyl group, which has a profound implication on the selectivity control. It can be expected that this conformation will be preserved in solution to some extent, owing to the rigidity of the amide bond.[12c]

Asymmetric induction pathway: On the basis of the absolute configurations of the products observed in the experiment, the crystal structure of the complex [Rh(2*R*,3*R*,5*S*,6*S*,2′*R*,3′*R*,5′*S*,6′*S*)-**10b**(acac)] (Figure 1), and the assumption that the selectivity-determining transition state (alkene insertion into the Rh–H bond) would adopt a trigonal-bipyramidal coordination geometry with equatorial and axial phosphorus atoms (since the bite angle of P1-Rh-P1A here (84.42(9)°) is close to 90°), the plausible models for asymmetric induction in the hydroformylation of terminal olefin derivatives with the present catalyst system are proposed. As can be seen from the crystal structure of the complex [Rh(2*R*,3*R*,5*S*,6*S*,2′*R*,3′*R*,5′*S*,6′*S*)-**10b**(acac)], the phenyl moieties A and C extend more significantly away from the plane defined by the phenyl backbone of the ligand than phenyl moieties B and D (see Figure 1). Accordingly, the steric environment developed by the ligands can be depicted with a simplified model shown in Scheme 5. Obviously, the transition-state model (a) is more favorable than (b), since the steric congestion between the equatorially coordinated olefin and the phenyl moiety **A** of the equatorial P atom in model (a) is less serious than that of the equatorial olefin

 © 2008 Wiley-VCH Verlag GmbH & Co. KGaA, Weinheim

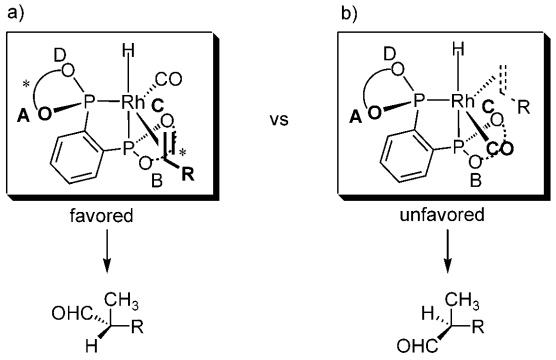

Scheme 5. The proposed asymmetric induction pathway for Rh^I-catalyzed AHF of terminal olefin derivatives.

with the phenyl moiety **C** of the axial P atom in model (b). In the favored transition state model (a), the R group of the olefin substrates at the equatorial position of the Rh complex will extend to the less hindered equatorial CO moiety. On the basis of this transition model, the absolute configurations of the branched hydroformylation products of vinyl acetate, styrene, and allyl cyanide will be S, *R*, and *R*, respectively. In fact, the absolute configurations of the corresponding products attained in the catalysis with ligand (2*R*,3*R*,5*S*,6*S*,2′*R*,3′*R*,5′*S*,6′*S*)-**10b** support the prediction mentioned above, which indicates that the formal addition of formaldehyde across the C=C double bond occurs at the same enantioface for all substrates. Moreover, the sense of asymmetric induction expected according to this model with all ligands **9**–**10** is consistent with that observed in the experiments except for the reaction of styrene under the catalysis of the Rh^I/**10d** complex (Table 3, entry 4). In this case, the Me groups at the *ortho* position of phenoxy moieties (B and D rings) probably have caused subtle changes in the steric hindrance of the ligand, and as a result influence the coordination of the olefin substrates, leading to changes of reactivity and the sense of asymmetric induction. In fact, relatively low catalytic activity was observed with the Rh^I complex of the ligand **10d**.

Conclusion

In summary, a new class of C_2-symmetric chiral bidentate phosphonite ligands has been developed and successfully applied to the Rh^I-catalyzed AHF of vinyl acetate, allyl cyanide, styrene, and its derivatives with high efficiency. The X-ray structural analysis of the catalyst precursor suggested that the steric hindrance caused by the protrusion of the remote substituents of the ligands into the vicinity of the metal center might be an important factor for the enantiocontrol of the catalysis, whereas the sense of the asymmetric induction can be rationalized on the basis of a trigonal-bipyramidal transition state diagram. The salient features of this type of ligands, such as cheap starting material, facile preparation, air-stability, structural diversity as well as the remote stereocontrol capability of the backbone substituents, will stimulate future studies to explore their applications in other transition-metal-catalyzed asymmetric reactions.

Experimental Section

General comments: All the experiments that were sensitive to moisture or air were carried out under an argon atmosphere using standard Schlenk techniques. NMR spectra were recorded in $CDCl_3$ or [D_6]DMSO on a Varian Mercury 300 (^{1}H 300 MHz; ^{13}C 75 MHz; ^{31}P 121 MHz) spectrometer. Chemical shifts are expressed in ppm with an internal standard: TMS (0 ppm), $CDCl_3$ ($\delta = 7.26$ ppm), and [D_6]DMSO ($\delta = 2.50$ ppm) for ^{1}H, and $CDCl_3$ ($\delta = 77.0$ ppm) and [D_6]DMSO ($\delta = 39.5$ ppm) for ^{13}C. ^{31}P NMR spectra were recorded with 85% H_3PO_4 as an external reference. The IR spectra were measured on a Rio-Rad FTS-185 spectrometer in KBr pellets. EI (70 eV) and ESI mass spectra were obtained on HP5989 A and Mariner LC-TOF spectrometers, respectively. HR-MS were determined on an IonSpect 4.7 TESLA FTMS. Elemental analyses were performed with an Elemental VARIO EL apparatus. Optical rotations were measured on a Perkin–Elmer 341 automatic polarimeter. HPLC analyses were carried out on a JASCO 1580 liquid chromatograph with a JASCO CD-1595 detector and AS-1555 autosampler. GC analyses were measured on Agilent 6890N system. *trans*-1*S*,2*S*-Diaminocyclohexane was obtained by optical resolution with tartaric acid,[14] and 3-methylsalicylaldehyde, 4-methylsalicylaldehyde, and 5-methylsalicylaldehyde were prepared by following the literature method.[15] The key intermediate diphenol (*R*,*R*)-**11** was synthesized from (1*R*,2*R*)-1,2-bis(2-methoxyphenyl)ethane-1,2-diamine according a literature procedure,[12a–b] and **14a–e** were prepared from (1*S*, 2*S*)-1,2-diaminocyclohexane and various salicylaldehyde derivatives by a three-step reaction sequence developed previously in our laboratory.[12c] 1,2-Bis(dichlorophosphino)ethane (**12**) is commercially available. 1,2-Bis(dichlorophosphino)benzene (**13**) was prepared by a modified literature procedure reported by Reetz et al.[16] (see Supporting Information). Dichloromethane was freshly distilled from calcium hydride; 2-propanol from magnesium filings; THF, benzene, *t*BuOMe, and toluene from sodium benzophenone ketyl; ethyl acetate and acetonitrile from P_2O_5.

Ligand synthesis

Preparation of (3*R*,4*R*,3′*R*,4′*R*)-9a: A solution of diphenol (*R*,*R*)-**11** (324 mg, 0.72 mmol) and Et_3N (0.20 mL, 1.44 mmol) in dry THF was added dropwise to a solution of 1,2-bis(dichlorophosphino)ethane (**12**; 83.5 mg, 0.36 mmol) in dry toluene (1.0 mL) at room temperature over 20 min, and the resulting mixture was stirred overnight. The reaction mixture was concentrated under reduced pressure, and the residue was purified by flash column chromatography on silica gel with chloroform/ethyl acetate (20/1) as eluent to give the corresponding bidentate phosphonite ligand (3*R*,4*R*,3′*R*,4′*R*)-**9a** as a white solid in 66% yield. M.p. 180–182 °C; $[\alpha]_D^{20} = -414$ ($c = 0.5$, $CHCl_3$); ^{1}H NMR (300 MHz, $CDCl_3$): $\delta = 6.97$–7.32 (m, 32H), 6.82 (t, $J = 8.4$ Hz, 2H), 6.64 (d, $J = 8.1$ Hz, 2H), 5.34 (d, $J = 15.3$ Hz, 2H), 5.01 (d, $J = 15.6$ Hz, 2H), 4.45 (d, $J = 3.3$ Hz, 2H), 4.34 (d, $J = 3.3$ Hz, 2H), 3.86 (d, $J = 15.3$ Hz, 2H), 3.58 (d, $J = 15.3$ Hz, 2H), 1.81–1.85 (m, 2H), 1.62–1.69 ppm (m, 2H); ^{31}P NMR (121.46 MHz, $CDCl_3$): $\delta = 177.87$ ppm (s); IR (KBr pellet): $\tilde{\nu} = 3030$, 1699, 1601, 1584, 1481, 1452, 1268, 1219, 1203, 1094, 877 cm^{-1}.

Preparation of (3*R*,4*R*,3′*R*,4′*R*)-9b: A solution of 1,2-bis(dichlorophosphino)benzene (93.3 mg, 0.333 mmol) in dry toluene (1.0 mL) was added dropwise to a solution of diphenol (*R*,*R*)-**11** (300 mg, 0.67 mmol) and Et_3N (0.18 mL, 1.33 mmol) in dry THF at room temperature over 20 min, and the resulting mixture was stirred overnight. The reaction mixture was concentrated under reduced pressure, and the residue was purified by flash column chromatography on silica gel with chloroform/ethyl acetate (20/1) as eluent to give the corresponding bidentate phosphonite ligand (3*R*,4*R*,3′*R*,4′*R*)-**9b** as a white solid in 71% yield. M.p. 132–134 °C; $[\alpha]_D^{20} = -142$ ($c = 0.5$, $CHCl_3$); ^{1}H NMR (300 MHz, $CDCl_3$): $\delta = 6.96$–7.38 (m, 36H), 6.72 (t, $J = 8.3$ Hz, 2H), 5.83 (d, $J = 7.8$ Hz, 2H), 5.32 (d, $J =$

 © 2008 Wiley-VCH Verlag GmbH & Co. KGaA, Weinheim

15.3 Hz, 2H), 5.05 (d, J=15.3 Hz, 2H), 4.65 (d, J=3.3 Hz, 2H), 4.50 (d, J=3.3 Hz, 2H), 3.89 (d, J=15.0 Hz, 2H), 3.60 ppm (d, J=15.6 Hz, 2H); ^{31}P NMR (121.46 MHz, $CDCl_3$): δ=150.58 ppm (s); IR (KBr pellet): $\tilde{\nu}$= 3030, 2919, 1700, 1602, 1584, 1481, 1453, 1267, 1216, 1093, 875, 771, 699 cm^{-1}; ESI-MS: m/z: 1035.4 ([M+H$^+$]); HRMS (MALDI/DHB): m/z: calcd for $C_{64}H_{53}N_4O_6P_2$ ([M+H$^+$]): 1035.3434; found: 1035.3443.

A typical procedure for the preparation of diphenol 14: The syntheses of key diphenol intermediates **14a–e** were reported in previous work.[12c] The preparation of **14f–l** were carried out by following a similar procedure. A typical procedure for the synthesis of **14a** was as follows: a solution of salicylaldehyde (46.4 g, 0.38 mol) in EtOH (200 mL) was added dropwise to a solution (400 mL) of *trans*-1*S*,2*S*-diaminocyclohexane (21.7 g, 0.19 mol) in ethanol at room temperature over 1 h. After stirring at reflux temperature for 12 h, the mixture was cooled to room temperature and the solvent was removed by vacuum evaporation. The oil-like residue was dissolved in a mixture of dry acetonitrile (1700 mL) and toluene (190 mL). To this solution was added manganese powder[17,12c] (325 mesh; 20.9 g, 0.38 mol), and the resulting mixture was cooled to 0 °C before trifluoroacetic acid (58.3 mL, 0.76 mol) was added dropwise over a period of 30 min under an Ar atmosphere. The reaction mixture was stirred vigorously at 20 °C for 24 h followed by addition of two additional equivalents of trifluoroacetic acid at 0 °C. After the mixture was left to stand at that temperature for 2 h, the resulting mixture was filtered and the residue was washed with petroleum ether (b.p. 60–90 °C, 2×50 mL) to afford a white solid. The solid was dissolved in H_2O (100 mL) and neutralized with saturated $NaHCO_3$ solution to pH 8. The aqueous solution was extracted with dichloromethane (3×200 mL). The combined organic layer was washed with H_2O (100 mL), dried over anhydrous Na_2SO_4, and concentrated. The resulting white solid was recrystallized with a mixture of petroleum and ethyl acetate (1:1) to afford the desired aminophenol compound as colorless needles in 85% yield (52.3 g). M.p. 226–227 °C (Lit. [15] m.p. 215 °C); $[\alpha]_D^{20}$=−5.5 (c=1.00, $CHCl_3$) [Lit. [15] $[\alpha]_D^{20}$=−7.2 (c=1.7, $CHCl_3$)]; ^{1}H NMR (300 MHz, $CDCl_3$): δ=1.41–1.46 (m, 4H), 1.76–1.82 (m, 4H), 2.41 (br, 2H), 2.67–2.70 (m, 2H), 4.15 (s, 2H), 6.12 (dd, J=1.8, 7.5 Hz, 2H), 6.42 (dt, J=1.2, 7.5 Hz, 2H), 6.83 (dd, J=1.2, 8.1 Hz, 2H,), 7.07 (dt, J=1.8, 7.8 Hz, 2H,), 10.86 ppm (br. s, 2H); ^{13}C NMR (75 MHz, $CDCl_3$): δ=156.7, 130.0, 128.8, 123.1, 118.4, 116.4, 63.2, 59.5, 31.4, 24.2 ppm; EI-MS: m/z: 324 ([M^+], 11), 203 (43), 122 (100).

To a solution of the above-prepared aminophenol compound (1.0 g, 3.1 mmol) and NEt_3 (1.72 mL, 12.3 mmol) in dry toluene (8 mL), benzoyl chloride (1.42 mL, 12.3 mmol) was added dropwise at room temperature over 10 min. The reaction mixture was stirred at 60 °C overnight. After removal of toluene under reduced pressure, 20% KOH aqueous solution (15 mL) and ethanol (15 mL) were added. After the mixture had been stirred at room temperature for 6 h, ethanol was removed under vacuum, and the resulting residue was neutralized with 6 N HCl aqueous solution to pH 8–9. The resulting solid was collected by filtration, washed with water (3×30 mL), and dried under vacuum. The desired compound (2*S*,3*S*,5*R*,6*R*)-**14a** (1.6 g) was obtained in 97% yield as a white solid, which could be used directly for the next step without further purification.

(2*R*,3*R*,5*S*,6*S*)-14a: Colorless prisms, Yield=97%, m.p. 264–265 °C; $[\alpha]_D^{20}$=+15.6 (c=1.00, CH_3OH); ^{1}H NMR (300 MHz, $CDCl_3$): δ=1.56–1.79 (m, 8H), 2.77 (br, 2H), 4.12 (br, 2H), 5.61 (br, 2H), 6.60 (d, J= 8.1 Hz, 2H), 6.87 (d, J=7.2 Hz, 4H), 7.02–7.09 (m, 6H), 7.16–7.24 (m, 4H), 7.63 ppm (d, J=7.5 Hz, 2H); ^{13}C NMR (75 MHz, [D$_6$]DMSO): δ= 173.1, 154.0, 136.6, 129.9, 128.6, 128.1, 127.9, 126.5, 126.0, 118.8, 115.2, 60.6, 55.1, 31.1, 24.9 ppm; IR (KBr): $\tilde{\nu}$=3236, 2934, 1625, 1602, 1579, 1485, 1388, 1337, 1239, 1110, 905, 755, 701 cm^{-1}; EI-MS: m/z: 532 ([M]$^+$, 2.7), 427 (11.5), 306 (5.5), 105 (100); HRMS (MALDI/DHB): m/z: calcd for $C_{34}H_{32}N_2O_4Na$ ([M + Na$^+$]): 555.2254; found: 555.2272; elemental analysis (%) calcd for $C_{34}H_{32}N_2O_4$: C 76.67, H 6.06, N 5.26; found: C 76.42, H 6.09, N 5.04.

The key intermediates **14f–l** were prepared in good to excellent yields by following a similar procedure mentioned above. Their characterization data are summarized as follows.

(2*S*,3*S*,5*R*,6*R*)-14f: Yield=76% ; white solid; m.p. 256–258 °C; $[\alpha]_D^{20}$= −77.0 (c=0.5, DMF); ^{1}H NMR (300 MHz, [D$_6$]DMSO): δ=1.51–1.37 (m, 4H), 1.75 (s, 2H), 2.23 (s, 6H), 2.29 (s, 6H), 2.69 (d, J=8.1 Hz, 2H), 3.88 (d, J=4.5 Hz, 2H), 5.86 (s, 2H), 6.54 (s, 2H), 6.77 (d, J=7.8 Hz, 2H), 6.90 (d, J=7.2 Hz, 4H), 7.01 (d, J=8.1 Hz, 4H), 7.54 (d, J=7.5 Hz, 2H), 8.94 ppm (s, 2H); ^{13}C NMR (75 MHz, [D$_6$]DMSO): δ=172.7, 153.4, 138.9, 137.0, 133.4, 127.9, 127.6, 126.1, 122.9, 119.1, 115.2, 60.2, 54.5, 30.7, 24.5, 20.4, 20.3 ppm; IR (KBr): $\tilde{\nu}$=3422, 2928, 2861, 1608, 1419, 1336, 1113, 831 cm^{-1}; ESI-MS: m/z: 589.2 ([M+H$^+$]); HRMS (MALDI/DHB): m/z: calcd for $C_{38}H_{41}N_2O_4$ ([M+H$^+$]): 589.3061; found: 589.3064.

(2*S*,3*S*,5*R*,6*R*)-14g: Yield=90%; white solid; m.p. 266–268 °C; $[\alpha]_D^{20}$= −58.0 (c=0.3, DMF); ^{1}H NMR (300 MHz, [D$_6$]DMSO): δ=1.23–1.78 (m, 6H), 2.06 (s, 12H), 2.32 (s, 6H), 2.68 (s, 2H), 3.84 (s, 2H), 5.76 (s, 2H), 6.55 (s, 6H), 6.78–6.92 (m, 4H), 7.50 (s, 2H), 8.92 ppm (s, 2H); ^{13}C NMR (75 MHz, [D$_6$]DMSO): δ=173.0, 153.5, 137.0, 136.1, 130.5, 127.6, 124.0, 122.9, 118.9, 115.2, 66.6, 59.9, 54.9, 30.0, 24.4, 20.4, 20.3 ppm; IR (KBr): $\tilde{\nu}$=2919, 1653, 1628, 1614, 1420, 1342, 1331, 1117, 863, 821 cm^{-1}; ESI-MS: m/z: 617.3 ([M+H$^+$]); elemental analysis (%) calcd for $C_{40}H_{44}N_2O_4$: C 77.89, H 7.19, N 4.54; found: C 77.47, H 7.54, N 4.16.

(2*S*,3*S*,5*R*,6*R*)-14h: Yield=90%; white solid; m.p. 180–182 °C; $[\alpha]_D^{20}$= −56.6 (c=0.5, $CHCl_3$); ^{1}H NMR (300 MHz, $CDCl_3$): δ=1.23 (d, J= 6.3 Hz, 12H), 1.43–1.73 (m, 6H), 2.81–2.68 (m, 4H), 4.08 (s, 2H), 5.54 (d, J=4.8 Hz, 2H), 6.48 (s, 2H), 6.82–7.17 (m, 14H), 7.46 ppm (s, 2H); ^{13}C NMR (75 MHz, $CDCl_3$): δ=175.2, 152.5, 150.3, 135.6, 130.2, 128.0, 126.8, 126.5, 122.7, 118.6, 114.1, 56.7, 33.6, 32.3, 25.0, 23.9, 23.8 ppm; IR (KBr): $\tilde{\nu}$=3441, 2959, 2932, 1624, 1426, 1339 cm^{-1}; ESI-MS: m/z: 617.3 ([M+H$^+$]); elemental analysis (%) calcd for $C_{40}H_{44}N_2O_4$: C 77.89, H 7.19, N 4.54; found: C 77.67, H 7.04, N 4.22.

(2*S*,3*S*,5*R*,6*R*)-14i: Yield=98%; white solid; m.p. 190–192 °C; $[\alpha]_D^{20}$= −20.2 (c=0.5, DMF); ^{1}H NMR (300 MHz, $CDCl_3$): δ=1.33 (s, 18H), 1.53–1.40 (m, 4H), 1.74 (s, 2H), 2.69 (br, 2H), 3.37 (s, 2H), 3.86 (s, 2H), 5.86 (s, 2H), 6.76 (s, 2H), 6.97 (s, 4H), 7.34–7.16 (m, 6H), 7.55 (s, 2H), 8.92 ppm (s, 2H); ^{13}C NMR (75 MHz, $CDCl_3$): δ=172.7, 153.2, 150.5, 136.3, 129.3, 127.4, 127.1, 126.0, 122.8, 114.8, 112.0, 60.0, 54.9, 33.6, 30.8, 30.5, 24.3 ppm; IR (KBr): $\tilde{\nu}$=3422, 2963, 1619, 1578, 1415, 1338 cm^{-1}; ESI-MS: m/z: 645.3 ([M+H$^+$]); elemental analysis (%) calcd for $C_{42}H_{48}N_2O_4$: C 78.23, H 7.50, N 4.34; found: C 78.34, H 7.66, N 4.19.

(2*R*,3*R*,5*S*,6*S*)-14j: Yield=99% ; white solid; m.p. 294–295 °C; $[\alpha]_D^{20}$= +107 (c=0.3, THF); ^{1}H NMR (300 MHz, [D$_6$]DMSO): δ=1.39–1.53 (m, 4H), 1.73 (br, 2H), 2.65 (d, J=10.2 Hz, 2H), 3.83 (d, J=5.1 Hz, 2H), 5.89 (s, 2H), 6.74 (d, J=7.8 Hz, 2H), 6.99–6.92 (m, 6H), 7.19 (t, J= 7.2 Hz, 2H), 7.29 (d, J=8.7 Hz, 4H), 7.64 (d, J=6.9 Hz, 2H), 9.18 ppm (s, 2H); ^{13}C NMR (75 MHz, [D$_6$]DMSO): δ=171.6, 153.4, 134.7, 134.2, 128.3, 127.8, 127.7, 127.6, 125.1, 118.5, 114.8, 60.1, 54.7, 30.6, 24.4 ppm; IR (KBr): $\tilde{\nu}$=3430, 2935, 1623, 1597, 1458, 1336, 1091, 837, 755 cm^{-1}; ESI-MS: m/z: 601.3 ([M+H$^+$]); elemental analysis (%) calcd for $C_{34}H_{30}Cl_2N_2O_4$: C 67.89, H 5.03, N 4.66; found: C 67.94, H 5.24, N 4.41.

(2*R*,3*R*,5*S*,6*S*)-14k: Yield=99%; white solid; m.p. 280–282 °C; $[\alpha]_D^{20}$= +68.6 (c=0.5, DMF); ^{1}H NMR (300 MHz, [D$_6$]DMSO): δ=1.37–1.50 (m, 4H), 1.72 (s, 2H), 2.61 (d, J=6.9 Hz, 2H), 3.66 (s, 6H), 3.86 (d, J= 6.3 Hz, 2H), 6.01 (s, 2H), 6.73–6.69 (m, 6H), 6.98–6.93 (m, 6H), 7.16 (t, J=7.2 Hz, 2H), 7.66 (d, J=7.2 Hz, 2H), 9.09 ppm (s, 2H); ^{13}C NMR (75 MHz, [D$_6$]DMSO): δ=172.3, 160.0, 153.6, 128.2, 128.0, 127.9, 127.7, 125.8, 118.3, 114.7, 112.7, 60.4, 54.6, 30.7, 24.4 ppm; IR (KBr): $\tilde{\nu}$=3245, 2934, 1604, 1511, 1458, 1335, 1253, 1174, 840 cm^{-1}; ESI-MS: m/z: 593.3 ([M+H$^+$]); elemental analysis (%) calcd for $C_{36}H_{36}N_2O_4$: C 72.95, H 6.12, N 4.73; found: C 72.86, H 6.00, N 4.42.

(2*R*,3*R*,5*S*,6*S*)-14l: Yield=98%; white solid; m.p. 272–274 °C; $[\alpha]_D^{20}$= +52.4 (c=1.0, CH_3OH); ^{1}H NMR (300 MHz, [D$_6$]DMSO): δ=1.15 (s, 18H), 1.48–1.36 (m, 4H), 1.62 (s, 2H), 2.65 (br, 2H), 4.04 (s, 2H), 5.87 (s, 2H), 6.57 (d, J=8.1 Hz, 2H), 7.00–6.92 (m, 6H), 7.16–7.10 (m, 6H), 7.59 ppm (s, 2H); ^{13}C NMR (75 MHz, $CDCl_3$): δ=175.3, 153.6, 152.8, 132.8, 129.1, 127.3, 126.7, 125.5, 125.0, 120.4, 116.3, 56.3, 34.6, 32.1, 31.0, 24.8 ppm; IR (KBr): $\tilde{\nu}$=33352, 3287, 2962, 2866, 1658, 1626, 1457, 1408, 1336, 1292, 754 cm^{-1}; ESI-MS: m/z: 645.3 ([M+H$^+$]); elemental analysis (%) calcd for $C_{42}H_{48}N_2O_4$: C 78.23, H7.50, N 4.34; found: C 77.62, H 7.43, N 4.02.

 © 2008 Wiley-VCH Verlag GmbH & Co. KGaA, Weinheim

Typical procedure for preparation of 10: The preparation of (2*R*,3*R*,5*S*,6*S*, 2′*R*,3′*R*,5′*S*,6′*S*)-**10a** was described here as a typical procedure. A solution of 1,2-bis(dichlorophosphino)benzene (125 mg, 0.446 mmol) in dry toluene (1.6 mL) was added dropwise to a solution of diphenol (2*R*,3*R*,5*S*,6*S*)-**14a** (500 mg, 0.892 mmol) and Et_3N (0.25 mL, 1.784 mmol) in dry THF at room temperature over 20 min, and the resulting mixture was stirred overnight. The reaction mixture was concentrated under the reduced pressure, and the residue was purified by flash column chromatography on silica gel with chloroform/ethyl acetate (20/1) as eluent to give the corresponding bidentate phosphonite ligands (2*R*,3*R*,5*S*,6*S*,2′*R*,3′*R*,5′*S*,6′*S*)-**10a** in 62% yield as a white solid. M.p. 212–214°C; $[\alpha]_D^{20}=+194$ ($c=0.5$, $CHCl_3$); ^{1}H NMR (300 MHz, $CDCl_3$): $\delta=$ 7.73–7.77 (m, 2H), 7.58 (d, $J=7.8$ Hz, 2H), 6.91–7.34 (m, 32H), 6.63–6.66 (m, 2H), 6.14 (d, $J=7.8$ Hz, 2H), 5.84 (s, 2H), 5.52 (t, $J=3.3$ Hz, 2H), 4.37–4.41 (m, 2H), 4.20–4.27 (m, 2H), 3.03–3.07 (m, 2H), 2.34–2.37 (m, 2H), 1.50–1.98 ppm (m, 12H); ^{31}P NMR (121.46 MHz, $CDCl_3$): $\delta=$ 151.82 ppm (s); ^{13}C NMR (75 MHz, CDCl3): $\delta=$175.9, 175.0, 152.04, 152.00, 151.96, 149.9, 143.6, 137.1, 136.3, 135.8, 133.0, 130.7, 130.2, 129.7, 129.0, 128.2, 128.1, 127.9, 127.7, 126.8, 126.7, 125.9, 125.2, 124.8, 124.5, 122.1, 121.4, 63.9, 59.4, 57.7, 57.5, 32.6, 31.8, 25.5, 24.7 ppm; IR (KBr pellet): $\tilde{\nu}=$3062, 2931, 1656, 1602, 1580, 1477, 1454, 1326, 1215, 1108, 1093, 874, 699 cm^{-1}; ESI-MS: *m/z*: 1199.7 ([*M*+H$^+$]); HRMS (MALDI/DHB): *m/z* calcd for $C_{74}H_{65}N_4O_8P_2$ ([*M*+H$^+$]): 1199.4272; found: 1199.4263.

Following a similar procedure for the preparation of **10a**, ligands **10b–l** were synthesized in moderate to good yields. Their characterization data are summarized as follows.

(2*R*,3*R*,5*S*,6*S*,2′*R*,3′*R*,5′*S*,6′*S*)-10b: Yield=62%; white solid; m.p. 214–216°C; $[\alpha]_D^{20}=+246$ ($c=0.36$, $CHCl_3$); ^{1}H NMR (300 MHz, $CDCl_3$): $\delta=$ 7.71–7.74 (m, 2H), 7.56 (d, $J=7.8$, 1.5 Hz, 2H), 7.30–7.32 (m, 4H), 6.68–7.14 (m, 24H), 6.63–6.66 (m, 2H), 6.11 (d, $J=8.1$ Hz, 2H), 5.87 (s, 2H), 5.46–5.52 (m, 2H), 4.37–4.41 (m, 2H), 4.17–4.21 (m, 2H), 3.02–3.06 (m, 2H), 2.25–2.29 (m, 2H), 2.24(s, 12H), 1.48–1.90 ppm (m, 12H); ^{31}P NMR (121.46 MHz, $CDCl_3$): $\delta=$150.24 ppm (s); ^{13}C NMR (75 MHz, $CDCl_3$): $\delta=$176.0, 175.1, 151.8, 149.8, 143.7, 140.7, 139.8, 135.9, 134.4, 133.4, 130.1, 128.9, 128.7, 128.4, 127.8, 127.5, 126.9, 126.8, 125.8, 125.1, 124.7, 124.4, 121.9, 121.4, 63.7, 59.3, 57.6, 57.5, 32.7, 31.7, 25.5, 24.6, 21.4, 21.3 ppm; IR (KBr pellet): $\tilde{\nu}=$2926, 1652, 1611, 1581, 1477, 1454, 1409, 1318, 1214, 1106, 874, 757 cm^{-1}; ESI-MS: *m/z*: 1254.8 ([*M*+H$^+$]); elemental analysis (%) calcd for $C_{78}H_{72}N_4O_8P_2$: C 74.63, H 5.78, N 4.46; found: C 74.43, H 6.07, N 4.16.

(2*R*,3*R*,5*S*,6*S*,2′*R*,3′*R*,5′*S*,6′*S*)-10c: Yield=66%; white solid; m.p. 168–170°C; $[\alpha]_D^{20}=+194$ ($c=0.3$, $CHCl_3$); ^{1}H NMR (300 MHz, $CDCl_3$): $\delta=$ 7.73–7.76 (m, 2H), 7.57 (d, $J=7.8$ Hz, 2H), 7.30–7.34 (m, 4H), 7.11–7.20 (m, 4H), 6.88–6.99 (m, 8H), 6.71–6.75 (m, 2H), 6.62 (s, 4H), 6.49 (s, 4H), 6.12 (d, $J=8.1$ Hz, 2H), 5.79 (s, 2H), 5.38–5.42 (m, 2H), 4.33–4.40 (m, 2H), 4.17–4.25 (m, 2H), 3.07–3.12 (m, 2H), 2.33–2.36 (m, 2H), 2.11 (s, 12H), 2.02 (s, 12H), 1.50–1.98 ppm (m, 12H); ^{31}P NMR (121.46 MHz, $CDCl_3$): $\delta=$151.52 ppm (s); ^{13}C NMR (75 MHz, $CDCl_3$): $\delta=$176.1, 175.2, 151.9. 151.8, 149.7, 143.9, 137.7, 137.6, 137.5, 137.2, 136.2, 136.0, 133.4, 132.2, 131.0, 129.9, 128.8, 127.6, 127.5, 125.9, 125.2, 124.6, 124.4, 124.3, 121.7, 121.0, 63.3, 59.1, 57.7, 57.6, 32.7, 31.6, 25.5, 24.7, 21.1, 20.9, 20.8 ppm; IR (KBr pellet): $\tilde{\nu}=$2927, 2863, 1656, 1604, 1582, 1477, 1454, 1333, 1253, 1220, 1170, 875, 763 cm^{-1}; ESI-MS: *m/z*: 1311.2 ([*M*+H$^+$]); HRMS (MALDI/DHB): *m/z* calcd for $C_{82}H_{81}N_4O_8P_2$ ([*M*+H$^+$]): 1311.5524; found: 1311.5550.

(2*S*,3*S*,5*R*,6*R*,2′*S*,3′*S*,5′*R*,6′*R*)-10d: Yield=74%; white solid; m.p. 238–240°C; $[\alpha]_D^{20}=-61.9$ ($c=0.5$, $CHCl_3$); ^{1}H NMR (300 MHz, $CDCl_3$): $\delta=$ 7.55 (d, $J=6.9$ Hz, 2H), 7.36–7.48 (m, 6H), 7.10–7.26 (m, 14H), 6.94 (d, $J=7.5$ Hz, 4H), 6.89 (t, $J=7.5$ Hz, 4H), 6.66 (d, $J=7.5$ Hz, 4H), 6.44 (t, $J=7.5$ Hz, 2H), 6.07 (s, 2H), 5.63 (t, $J=6.3$ Hz, 2H), 4.44 (t, $J=9.9$ Hz, 2H), 4.04 (t, $J=10.2$ Hz, 2H), 3.03 (d, $J=12.3$ Hz, 2H), 2.57 (d, $J=$ 11.1 Hz, 2H), 1.48–1.90 ppm (m, 24H); ^{31}P NMR (121.46 MHz, $CDCl_3$): $\delta=$156.16 ppm (s); ^{13}C NMR (75 MHz, $CDCl_3$): $\delta=$176.6, 174.2, 151.0, 150.2, 144.8, 136.5, 136.0, 134.6, 130.7, 130.4, 130.3, 130.1, 130.0, 129.9, 129.7, 129.0, 128.5, 128.0, 127.1, 126.9, 125.4, 124.2, 124.1, 123.9, 123.2, 77.2, 65.5, 58.3, 58.0, 56.6, 33.5, 32.5, 25.2, 24.9, 17.2, 16.9 ppm; IR (KBr pellet): $\tilde{\nu}=$3059, 2929, 1658, 1600, 1580, 1462, 1403, 1326, 1255, 1183, 1166, 1107, 888, 873, 757 cm^{-1}; ESI-MS: *m/z*: 1255.0 ([*M*+H$^+$]); elemental analysis (%) calcd for $C_{78}H_{72}N_4O_8P_2$: C 74.63, H 5.78, N 4.46; found: C 74.24, H 6.08, N 4.00.

(2*S*,3*S*,5*R*,6*R*,2′*S*,3′*S*,5′*R*,6′*R*)-10e: Yield=49%; white solid; m.p. 196–198°C; $[\alpha]_D^{20}=-191$ ($c=0.5$, $CHCl_3$); ^{1}H NMR (300 MHz, $CDCl_3$): $\delta=$ 7.58 (d, $J=7.5$ Hz, 2H), 7.42 (d, $J=7.5$ Hz, 2H), 6.91–7.30 (m, 26H), 6.82 (s, 2H), 6.69–6.72 (m, 2H), 5.98 (s, 2H), 5.80 (s, 2H), 5.46–5.49 (m, 2H), 4.31–4.35 (m, 2H), 4.21–4.26 (m, 2H), 3.03–3.07 (m, 2H), 2.36 (s, 6H), 2.32–2.35 (m, 2H), 2.08 (s, 6H), 1.50–1.98 ppm (m, 12H); ^{31}P NMR (121.46 MHz, $CDCl_3$): $\delta=$151.91 ppm (s); ^{13}C NMR (75 MHz, $CDCl_3$): $\delta=$175.9, 175.0, 151.94, 151.91, 151.88, 149.8, 143.8, 143.7, 139.1, 137.9, 137.2, 136.4, 132.8, 130.4, 129.9, 129.7, 129.6, 128.1, 127.8, 127.6, 127.5, 126.8, 126.7, 125.4, 125.3, 125.0, 124.8, 122.6, 122.1, 63.8, 59.2, 57.7, 57.4, 32.7,31.6, 25.5, 24.7, 21.0, 20.7 ppm; IR (KBr pellet): $\tilde{\nu}=$2928, 2860, 1657, 1617, 1496, 1447, 1403, 1326, 1244, 1108, 960, 786, 700 cm^{-1}; ESI-MS: *m/z*: 1255.4 ([*M*+H$^+$]); HRMS (MALDI/DHB): *m/z*: calcd for $C_{78}H_{73}N_4O_8P_2$ ([*M*+H$^+$]): 1255.4898; found: 1255.4898.

(2*S*,3*S*,5*R*,6*R*,2′*S*,3′*S*,5′*R*,6′*R*)-10f: Yield=33%; white solid; m.p. 206–208°C; $[\alpha]_D^{20}=-223.8$ ($c=0.5$, $CHCl_3$); ^{1}H NMR (300 MHz, $CDCl_3$): $\delta=$ 7.60 (d, $J=7.8$ Hz, 2H), 7.42 (d, $J=8.1$ Hz, 2H), 7.10–6.87 (m, 22H), 6.68 (s, 2H), 5.91 (s, 2H), 5.83 (s, 2H), 5.42 (s, 2H), 4.41 (t, $J=10.8$ Hz, 2H), 4.17 (t, $J=8.7$ Hz, 2H), 3.04 (d, $J=11.1$ Hz, 2H), 2.34 (s, 6H), 2.28 (s, 6H), 2.25 (s, 6H), 2.03 (s, 6H), 1.43–1.88 (m, 14H); ^{31}P NMR (121.46 MHz, $CDCl_3$): $\delta=$149.72 ppm (s); ^{13}C NMR (75 MHz, $CDCl_3$): $\delta=$175.9, 175.2, 151.8, 149.6, 144.0, 140.7, 139.7, 139.1, 137.6, 134.6, 133.5, 133.0, 130.4, 130.0, 128.7, 128.4, 127.4, 127.1, 126.9, 125.4, 125.3, 125.0, 124.6, 122.5, 122.0, 77.2, 63.8, 59.4, 57.7, 57.6, 32.8, 31.7, 25.6, 24.7, 21.5, 21.3, 20.9, 20.7 ppm; IR (KBr pellet): $\tilde{\nu}=$2925, 2859, 1654, 1614, 1403, 1325, 1243, 1107 cm^{-1}; HRMS (MALDI/DHB): *m/z*: calcd for $C_{82}H_{81}N_4O_8P_2$ ([*M*+H$^+$]): 1311.5524; found: 1311.5555.

(2*S*,3*S*,5*R*,6*R*,2′*S*,3′*S*,5′*R*,6′*R*)-10g: Yield=78%; white solid; m.p. 182–184°C; $[\alpha]_D^{20}=-174$ ($c=0.25$, $CHCl_3$); ^{1}H NMR (300 MHz, $CDCl_3$): $\delta=$ 7.60 (d, $J=7.5$ Hz, 2H), 7.43 (d, $J=7.5$ Hz, 2H), 7.22–7.19 (m, 2H), 7.13 (d, $J=7.5$ Hz, 2H), 6.93–6.90 (m, 8H), 6.78 (s, 2H), 6.64 (s, 4H), 6.52 (s, 4H), 5.91 (s, 2H), 5.73 (s, 2H), 5.35 (s, 2H), 4.34 (t, $J=11.1$ Hz, 2H), 4.18 (t, $J=8.7$ Hz, 2H), 3.70 (d, $J=1.5$ Hz, 2H), 3.11 (d, $J=11.4$ Hz, 2H), 2.36 (s, 6H), 2.12 (s, 12H), 2.05 (s, 6H), 2.03 (s, 12H), 1.72–1.85 ppm (m, 12H); ^{31}P NMR (121.46 MHz, $CDCl_3$): $\delta=$151.21 ppm (s); ^{13}C NMR (75 MHz, $CDCl_3$): $\delta=$176.2, 175.3, 151.9, 149.5, 138.9, 137.6, 137.5, 137.4, 137.3,136.1, 133.3, 132.1, 130.8, 130.4, 129.6, 125.6, 125.1, 125.0, 124.8, 124.6, 124.4, 122.3, 121.9, 63.3, 59.1, 57.8, 57.7, 43.4, 41.8, 32.8, 31.6, 26.9, 25.6, 24.8, 24.7, 21.1 ppm; IR (KBr pellet): $\tilde{\nu}=$2929, 1657, 1652, 1403, 1336, 1244 cm^{-1}; HRMS (MALDI/DHB): *m/z*: calcd for $C_{86}H_{89}N_4O_8P_2$ ([*M*+H$^+$]): 1367.6150; found: 1367.6171.

(2*S*,3*S*,5*R*,6*R*,2′*S*,3′*S*,5′*R*,6′*R*)-10h: Yield=27%; white solid; m.p. 179–181°C; $[\alpha]_D^{20}=-167.7$ (c 0.5, $CHCl_3$); ^{1}H NMR (300 MHz, $CDCl_3$) $\delta=$ 7.63 (d, $J=7.8$ Hz, 2H), 7.47 (d, $J=7.8$ Hz, 2H), 7.31–6.95 (m, 26H), 6.85 (s, 2H), 6.74 (s, 2H), 6.05 (s, 2H), 5.77 (s, 2H), 5.45 (s, 2H), 4.42 (t, $J=$ 8.1 Hz, 2H), 4.21 (t, $J=8.7$ Hz, 2H), 3.08 (d, $J=11.4$ Hz, 2H), 2.87–2.83 (m, 2H), 2.66–2.61 (m, 2H), 2.28 (d, $J=5.1$ Hz, 2H), 1.87–1.46 (m, 12H), 1.22 (d, $J=6.9$ Hz, 6H), 1.13 (d, $J=6.9$ Hz, 6H), 0.99 (d, $J=7.2$ Hz, 6H), 0.95 ppm (d, $J=6.9$ Hz, 6H); ^{31}P NMR (121.46 MHz, $CDCl_3$): $\delta=$ 150.96 ppm (s); ^{13}C NMR (75 MHz, $CDCl_3$): $\delta=$175.9, 175.0, 152.1, 150.4, 149.8, 148.8, 137.4, 136.5, 133.2, 130.6, 130.2, 129.6, 128.1, 127.9, 127.6, 126.9, 126.8, 125.5, 124.8, 123.0, 122.3, 119.8, 119.4, 109.7, 63.6, 59.5, 57.7, 33.7, 33.3, 32.8, 31.6, 25.6, 24.7, 23.9, 23.8, 23.6, 23.4 ppm; IR (KBr pellet): $\tilde{\nu}=$2960, 2930, 1655, 1407, 1328, 1110 cm^{-1}; HRMS (MALDI/DHB): *m/z*: calcd for $C_{86}H_{89}N_4O_8P_2$ ([*M*+H$^+$]): 1367.6150; found: 1367.6154.

(2*S*,3*S*,5*R*,6*R*,2′*S*,3′*S*,5′*R*,6′*R*)-10i: Yield=41%; white solid; m.p. 212–214°C; $[\alpha]_D^{20}=-126.6$ ($c=0.5$, $CHCl_3$); ^{1}H NMR (300 MHz, $CDCl_3$): $\delta=$ 7.64 (d, $J=7.8$ Hz, 2H), 7.49 (d, $J=7.8$ Hz, 2H), 7.32–6.95 (m, 28H), 6.96 (s, 2H), 6.22 (s, 2H), 5.78 (s, 2H), 5.44 (s, 2H), 4.43 (t, $J=7.2$ Hz, 2H), 4.21 (t, $J=7.8$ Hz, 2H), 3.07 (d, $J=10.5$ Hz, 2H), 2.29 (d, $J=7.2$ Hz, 2H), 1.87–1.44 (m, 12H), 1.19 (s, 18H), 1.04 ppm (s, 18H); ^{31}P NMR (121.46 MHz, $CDCl_3$): $\delta=$150.40 ppm (d, $J=24.6$ Hz); ^{13}C NMR (75 MHz, $CDCl_3$): $\delta=$175.9, 175.1, 152.9, 151.9, 151.2, 149.6, 137.5, 136.5, 132.7, 130.6, 130.2, 129.6, 128.1, 127.8, 127.0, 126.9, 125.2, 124.7, 121.4,

 © 2008 Wiley-VCH Verlag GmbH & Co. KGaA, Weinheim

120.9, 119.4, 118.8, 63.6, 59.5, 57.7, 34.7, 34.3, 32.9, 31.6, 31.1, 31.0, 25.6, 24.7 ppm; IR (KBr pellet): $\tilde{\nu}$ = 2962, 2865, 1655, 1402, 1327, 1213, 940 cm^{-1}; HRMS (MALDI/DHB): *m/z*: calcd for $C_{90}H_{97}N_4O_8P_2$ ([*M*+H^+]): 1423.6776; found: 1423.6733.

(2*R*,3*R*,5*S*,6*S*,2′*R*,3′*R*,5′*S*,6′*S*)-10j: Yield = 56%; white solid; m.p. 195–196 °C; $[\alpha]_D^{20}$ = +222.7 (*c* = 0.5, $CHCl_3$); ^1H NMR (300 MHz, $CDCl_3$): δ = 7.71 (d, *J* = 6.9 Hz, 2H), 7.53 (d, *J* = 7.5 Hz, 2H), 7.36–6.89 (m, 28H), 6.75 (s, 2H), 6.18 (d, *J* = 8.4 Hz, 2H), 5.79 (s, 2H), 5.52 (s, 2H), 4.39 (t, *J* = 10.5 Hz, 2H), 4.21 (t, *J* = 9.6 Hz, 2H), 3.05 (d, *J* = 11.4 Hz, 2H), 2.30 (s, 2H), 1.96–1.89 (m, 4H), 1.76–1.57 ppm (m, 8H); ^{31}P NMR (121.46 MHz, $CDCl_3$): δ = 150.86 ppm (s); ^{13}C NMR (75 MHz, $CDCl_3$): δ = 174.6, 173.7, 151.8, 149.6, 143.2, 136.4, 135.9, 135.7, 135.0, 134.5, 132.9, 130.8, 129.4, 128.5, 128.3, 128.1,127.4, 125.6, 124.8, 124.5, 122.1, 121.8, 63.8, 59.2, 57.6, 57.5, 56.6, 32.5, 31.6, 25.4, 24.6 ppm; IR (KBr pellet): $\tilde{\nu}$ = 2931, 1655, 1476, 1454, 1401, 1326, 1214, 1090, 874, 759 cm^{-1}; HRMS (MALDI/DHB): *m/z*: calcd for $C_{74}H_{61}Cl_4N_4O_8P_2$ ([*M*+H^+]): 1335.2713; found: 1335.2694.

(2*R*,3*R*,5*S*,6*S*,2′*R*,3′*R*,5′*S*,6′*S*)-10k: Yield = 45%; white solid; m.p. 198–200 °C; $[\alpha]_D^{20}$ = +225.4 (*c* = 0.4, $CHCl_3$); ^1H NMR (300 MHz, $CDCl_3$): δ = 7.76 (d, *J* = 5.4 Hz, 2H), 7.57 (d, *J* = 7.2 Hz, 2H), 7.36–6.63 (m, 30H), 6.16 (d, *J* = 7.8 Hz, 2H), 5.93 (s, 2H), 5.53 (s, 2H), 4.48 (t, *J* = 10.8 Hz, 2H), 4.22 (t, *J* = 10.8 Hz, 2H), 3.64 (s, 6H), 3.62 (s, 6H), 3.02 (d, *J* = 10.5 Hz, 2H), 2.31 (d, *J* = 6.3 Hz, 2H), 2.02–1.87 (m, 4H), 1.80–1.56 ppm (m, 8H); ^{31}P NMR (121.46 MHz, $CDCl_3$): δ = 150.41 ppm (s); ^{13}C NMR (75 MHz, $CDCl_3$): δ = 175.3, 174.6, 161.1, 160.6, 151.6, 149.5, 143.3, 135.7, 133.1, 129.9, 129.3, 128.7, 128.5, 128.4, 128.1, 127.5, 125.5, 124.9, 124.4, 124.1, 121.7, 121.2, 113.1, 112.8, 76.9, 63.7, 59.9, 59.3, 57.2, 54.9, 54.7, 32.3, 31.4, 25.2, 24.4 ppm; IR (KBr pellet): $\tilde{\nu}$ = 2932, 2858, 1649, 1606, 1325, 1303, 1253, 1173 cm^{-1}; HRMS (MALDI/DHB): *m/z*: calcd for $C_{78}H_{73}N_4O_8P_2$ ([*M*+H^+]): 1319.4695; found: 1319.4690.

(2*R*,3*R*,5*S*,6*S*,2′*R*,3′*R*,5′*S*,6′*S*)-10l: Yield = 50%; white solid; m.p. 160–162 °C; $[\alpha]_D^{20}$ = +245.5 (*c* = 0.5, $CHCl_3$); ^1H NMR (300 MHz, $CDCl_3$) δ = 7.74 (d, *J* = 4.5 Hz, 2H), 7.73 (d, *J* = 7.2 Hz, 2H), 7.31–6.68 (m, 30H), 6.10 (d, *J* = 7.8 Hz, 2H), 5.96 (s, 2H), 5.49 (s, 2H), 4.46 (t, *J* = 10.2 Hz, 2H), 4.15 (t, *J* = 10.8 Hz, 2H), 3.04 (d, *J* = 10.2 Hz, 2H), 2.25 (s, 2H), 1.86–1.52 (m, 12H), 1.23 (s, 18H), 1.15 ppm (s, 18H); ^{31}P NMR (121.46 MHz, $CDCl_3$): δ = 149.88 ppm (s); ^{13}C NMR (75 MHz, $CDCl_3$): δ = 176.0, 174.9, 153.8, 153.2, 151.9, 149.6, 143.6, 136.0, 134.5, 133.8, 133.3,130.0, 129.0, 127.8, 127.5, 127.0, 126.6, 125.6, 125.5, 124.9, 124.8, 124.7, 124.3, 121.8, 63.8, 59.4, 57.5, 34.6, 32.6, 31.6, 31.0, 29.5, 25.6, 24.6 ppm; IR (KBr pellet): $\tilde{\nu}$ = 2962, 1654, 1326, 1214, 875, 768 cm^{-1}; HRMS (MALDI/DHB): *m/z*: calcd for $C_{90}H_{97}N_4O_8P_2$ ([*M*+H^+]): 1423.6776; found: 1423.6809.

Preparation and X-ray crystallographic analysis of [(2*R*,3*R*,5*S*,6*S*,2′*R*,3′*R*,5′*S*,6′*S*)-10b][Rh(acac)]: [Rh(acac)$(CO)_2$] (9.5 mg, 0.0368 mmol) and (2*R*,3*R*,5*S*,6*S*,2′*R*,3′*R*,5′*S*,6′*S*)-**6b** (46.6 mg, 0.0368 mmol) were dissolved in dry chloroform (1 mL), and hexane (8 mL) was diffused into the solution by slow evaporation at room temperature. After one week, a large amount of single crystals was obtained as orange needles. X-ray crystallographic analysis was performed with a Bruker SMART CCD-APEX at 20 °C. $C_{83}H_{79}N_4O_{10}P_2Rh$, M_r = 1576.72, tetragonal, *P*4(3)2(1)2, *a* = 14.4686(6), *b* = 14.4686(6), *c* = 38.287(2) Å; *V* = 8015.1(6) $Å^3$, $1.50 < 2\theta < 27.50°$; ρ_{calcd} = 1.307 $g\,cm^{-3}$, *Z* = 4, R_{int} = 0.1369, goodness of fit indicator = 0.863, final *R*1 = 0.0625, *wR*2 = 0.1269 on F^2 for observed data, P_{max}, P_{min} = 0.604, −0.404 $Å^{-3}$; absolute structure parameter was 0.04(5). CCDC-678150 contains the supplementary crystallographic data for this paper. These data can be obtained free of charge from The Cambridge Crystallographic Data Centre via www.ccdc.cam.ac.uk/data_request/cif

General procedure for catalytic AHF: The styrene/vinyl acetate/dodecane solution was prepared by mixing styrene (21.58 g, 0.2075 mol) and vinyl acetate (17.85 g, 0.2075 mol) with dodecane (7.055 g, 0.0415 mol) (as a GC internal standard). The allyl cyanide/dodecane solution was prepared by mixing allyl cyanide (27.015 g, 0.403 mol) with (6.855 g, 0.0403 mol) in toluene (9.6 mL). [Rh(acac)$(CO)_2$] (1.1 mg, 0.0043 mmol) and ligand **10b** (8.0 mg, 0.0064 mmol) were dissolved in *t*BuOMe (0.45 mL) under an argon atmosphere, and the solution was stirred at room temperature for 10 min. The solution of the substrate prepared above was added to the catalyst solution in a glove box. The resulting mixture was then transferred to a stainless steel autoclave under an argon atmosphere, and then sealed. After autoclave had been purged with syngas (H_2/CO = 4:1) three times, the final pressure was adjusted to the appropriate value. The reactor was heated to the desired temperature while stirring at 800 rpm. The reaction was stopped after 2 or 4 h then cooled by using ice water, and then the syngas was released carefully. Upon opening the reactor, 0.1 mL of the reaction mixture was taken out and diluted with toluene (1.0 mL). This solution was analyzed by gas chromatography. For analysis of the products of the reactions of styrene and vinyl acetate, a Supelco's Beta Dex 225 column was used under a temperature program of 100 °C for 5 min, then 4 °C per min to 160 °C. Retention time: 2.35 min for vinyl acetate (**18**), 6.62 min for (*R*)-**19**, and 8.37 min for (*S*)-**19**, the enantiomers of the acetic acid 1-methyl-2-oxo-ethyl ester (branched regioisomer **19**), 11.28 min for acetic acid 3-oxo-propyl ester (linear regioisomer **20**); 4.59 min for styrene (**15a**), 12.11 min for (*R*)-**16a** and 12.34 min for (*S*)-**16a**, the enantiomers of 2-phenylpropionaldehyde (branched regioisomer **16a**), 16.08 min for 3-phenylpropionaldehyde (linear regioisomer **17a**), and 10.33 min for *n*-dodecane. For the analysis of reaction product of allyl cyanide, Supelco's Beta Dex 120 column was used under a temperature program of 80 °C for 5 min, then 10 °C per min to 130 °C. This method was applied to determine the conversion of substrate **21** and the b/l ratio in the products **22** and **23**. Retention time: 3.7 min for allyl cyanide (**21**), 11.75 min for 3-methyl-4-oxo-butyronitrile (branched regioisomer **22**), 13.61 min for 5-oxo-pentanenitrile (linear regioisomer **23**), and 12.49 min for *n*-dodecane. The enantiomeric excess of the product **22** was determined by GC analysis of its methyl ester on a Supelco's Beta Dex 120 column under a temperature program of 80 °C for 0 min, then 1 °C per min to 100 °C, 100 °C for 8 min, then 4 °C per min to 130 °C. Retention time: 26.3 min (*S*) and 26.6 min (*R*) for the enantiomers of the methyl-3-cyano-2-methylpropanoate (branched regioisomer). The methyl ester was obtained by oxidation with Jones reagent to give initially carboxylic acids, followed by esterification using CH_2N_2·Et_2O solution.

Acknowledgements

This work was supported by the National Natural Science Foundation of China (No. 20532050, 20632060), the Chinese Academy of Sciences, the Major Basic Research Development Program of China (Grant No. 2006CB806106), the Science and Technology Commission of Shanghai Municipality, and Merck Research Laboratories.

[1] For reviews, see: a) *Rhodium Catalyzed Hydroformylation*, Vol. 22, (Eds.: C. Claver, P. W. N. M. van Leeuwen), Kluwer Academic Publishers, Dordrecht, The Netherlands, **2000**; b) W. A. Herrmann, B. Cornils, *Angew. Chem.* **1997**, *109*, 1074–1095; *Angew. Chem. Int. Ed. Engl.* **1997**, *36*, 1048–1067; c) B. Breit, W. Seiche, *Synthesis* **2001**, 1–36; d) B. Breit, *Angew. Chem.* **2005**, *117*, 6976–6986; *Angew. Chem. Int. Ed.* **2005**, *44*, 6816–6825.

[2] For recent reviews on AHF, see: a) F. Agbossou, J. Carpentier, A. Mortreux, *Chem. Rev.* **1995**, *95*, 2485–2506; b) C. Claver, P. W. N. M. van Leeuwen, in *Rhodium Catalyzed Hydroformylation, Vol. 22*, (Eds.: C. Claver, P. W. N. M. van Leeuwen), Kluwer Academic Publishers, Dordrecht, The Netherlands, **2000**, chapter 5; c) M. Dieguez, O. Pamies, C. Claver, *Tetrahedron: Asymmetry* **2004**, *15*, 2113–2122; d) C. Claver, M. Dieguez, O. Pamies, S. Castillon, *Top. Organomet. Chem.* **2006**, *18*, 35–64; e) J. Klosin, C. R. Landis, *Acc. Chem. Res.* **2007**, *40*, 1251–1259; f) K. Nozaki, I. Ojima in *Catalytic Asymmetric Synthesis*, 2nd ed, (Ed.: I. Ojima), Wiley-VCH, New York, **2000**, chapter 7.

[3] a) J. K. Still in *Comprehensive Organic Synthesis, Vol. 4*, (Eds.: B. M. Trost, I. Flemming, L. A. Paquette), Pergamon Press, Oxford, **1991**, 913–950; for a recent example, see: b) Šmejkal, B. Breit, *Angew. Chem. Int. Ed.* **2008**, *47*, 311–315.

 © 2008 Wiley-VCH Verlag GmbH & Co. KGaA, Weinheim

[4] For examples, see: a) R. Noyori, *Asymmetric Catalysis in Organic Synthesis*, Wiley-Interscience, New York, **1994**; b) *Catalytic Asymmetric Synthesis*, 2nd ed. (Ed.: I. Ojima), Wiley-VCH, New York, **2000**; c) *Comprehensive Asymmetric Catalysis, Vol. I-III* (Eds.: E. N. Jacobsen, A. Pfaltz, H. Yamamoto), Springer, Berlin, **1999**; d) *Lewis Acids in Organic Synthesis*, (Ed.: H. Yamamoto), Wiley-VCH, New York, **2001**; e) *Asymmetric Catalysis on Industrial Scale: Challenges, Approaches and Solutions* (Eds.: H. U. Blaser, E. Schmidt), Wiley-VCH, Weinheim, **2004**; f) *New Frontiers in Asymmetric Catalysis* (Eds.: K. Mikami, M. Lautens), Wiley-VCH, **2007**.

[5] a) G. T. Whiteker, J. R. Briggs, J. E. Babin, B. A. Barne, *Asymmetric Catalysis Using Bisphosphite Ligands in Chemical Industries, Vol. 89*, Marcel Dekker, Inc., New York, **2003**, pp. 359–367; b) G. J. H. Buisman, E. J. Vos, P. C. J. Kamer, P. W. N. M. van Leeuwen, *J. Chem. Soc. Dalton Trans.* **1995**, 409–417; c) G. J. H. Buisman, L. A. van der Veen, A. Klootwijk, W. G. J. de Lange, P. C. J. Kamer, P. W. N. M. van Leeuwen, D. Vogt, *Organometallics* **1997**, *16*, 2929–2939; d) M. Dieguez, O. Pamies, A. Ruiz, S. Castillon, C. Claver, *Chem. Eur. J.* **2001**, *7*, 3086–3094.

[6] a) C. J. Cobley, K. Gardner, J. Klosin, C. Praquin, C. Hill, G. T. Whiteker, A. Zanotti-Gerosa, J. L. Petersen, K. A. Abboud, *J. Org. Chem.* **2004**, *69*, 4031–4040; b) C. J. Cobley, J. Klosin, C. Qin, G. T. Whiteker, *Org. Lett.* **2004**, *6*, 3277–3280; c) C. J. Cobley, R. D. J. Froese, J. Klosin, C. Qin, G. T. Whiteker, *Organometallics* **2007**, *26*, 2986–2999.

[7] S. Breeden, D. J. Cole-Hamilton, D. F. Foster, G. J. Schwarz, M. Wills, *Angew. Chem.* **2000**, *112*, 4272–4274; *Angew. Chem. Int. Ed.* **2000**, *39*, 4106–4108.

[8] a) N. Sakai, S. Mano, K. Nozaki, H. Takaya, *J. Am. Chem. Soc.* **1993**, *115*, 7033–7034; b) K. Nozaki, N. Sakai, T. Nanno, T. Higashijima, S. Mano, T. Horiuchi, H. Takaya, *J. Am. Chem. Soc.* **1997**, *119*, 4413–4423; c) F. Shibahara, K. Nozaki, T. Hiyama, *J. Am. Chem. Soc.* **1997**, *119*, 8555–8560; d) K. Nozaki, T. Matsuo, F. Shibahara, T. Hiyama, *Adv. Synth. Catal.* **2001**, *343*, 61–63; e) F. Shibahara, K. Nozaki, T. Hiyama, *J. Am. Chem. Soc.* **2003**, *125*, 8555–8560.

[9] Y. Yan, X. Zhang, *J. Am. Chem. Soc.* **2006**, *128*, 7198–7202.

[10] a) T. P. Clark, C. R. Landis, S. L. Freed, J. Klosin, K. Abboud, *J. Am. Chem. Soc.* **2005**, *127*, 5040–5042; b) P. J. Thomas, A. T. Axtell, J. Klosin, W. Peng, C. R. Rand, T. P. Clark, C. R. Landis, K. A. Abboud, *Org. Lett.* **2007**, *9*, 2665–2668.

[11] a) C. J. Cobley, J. Klosin, C. Qin, G. T. Whiteker, *Org. Lett.* **2004**, *6*, 3277–3280; b) A. T. Axtell, J. Klosin, K. A. Abboud, *Organometallics* **2006**, *25*, 5003–5009; c) A. T. Axtell, C. J. Cobley, J. Klosin, G. T. Whiteker, A. Zanotti-Gerosa, K. A. Abboud, *Angew. Chem.* **2005**, *117*, 5984–5988; *Angew. Chem. Int. Ed.* **2005**, *44*, 5834–5838.

[12] a) Y. Liu, K. Ding, *J. Am. Chem. Soc.* **2005**, *127*, 10488–10499; b) Y. Liu, C. A. Sandoval, Y. Yamaguchi, X. Zhang, Z. Wang, K. Kato, K. Ding, *J. Am. Chem. Soc.* **2006**, *128*, 14212–14213; c) B. Zhao, Z. Wang, K. Ding, *Adv. Synth. Catal.* **2006**, *348*, 1049–1057.

[13] a) K. Nozaki, T. Matsuo, F, Shibahara, T. Hiyama, *Organometallics* **2003**, *22*, 594–600; b) K. Nozaki in *New Frontiers in Asymmetric Catalysis*, (Ed.: K. Mikami, M. Lautens), Wiley-VCH, New York, **2007**, Chapter 4.

[14] J. F. Larrow, E. N. Jacobsen, *J. Org. Chem.* **1994**, *59*, 1939–1942.

[15] T. Shono, N. Kise, E. Shirakawa, H. Matsumoto, E. Okazaki, *J. Org. Chem.* **1991**, *56*, 3063–3067.

[16] a) M. T. Reetz, D. Moulin, A. Gosberg, *Org. Lett.* **2001**, *3*, 4083–4085; b) M. T. Reetz, A. Gosberg, *Tetrahedron: Asymmetry* **1999**, *10*, 2129–2137.

[17] N. U. Hofslokken, L. Skatteboel, *Acta. Chem. Scand.* **1999**, *53*, 258–262.

[18] a) G. Consiglio, P. Pino, L. I. Flowers Jr, C. U. Pittman, *J. Chem. Soc. Chem. Commun.* **1983**, 612–613; b) S. G. Cohen, J. Crossley, E. Khedouri, R. Zand, L. H. Klee, *J. Am. Chem. Soc.* **1963**, *85*, 1685–1691.

[19] Z.-F. Xie, H. Suemune, K. Sakai, *Tetrahedron: Asymmetry* **1993**, *4*, 973–980.

Received: March 4, 2008
Published online: July 15, 2008

 © 2008 Wiley-VCH Verlag GmbH & Co. KGaA, Weinheim